NMR and μSR study of spin correlations in $SrZnVO(PO_4)_2$: An $S = \frac{1}{2}$ frustrated magnet on a square lattice

L. Bossoni,[1] P. Carretta,[1] R. Nath,[2] M. Moscardini,[1] M. Baenitz,[3] and C. Geibel[3]
[1]*Department of Physics "A. Volta," University of Pavia-CNISM, I-27100 Pavia, Italy*
[2]*Indian Institute of Science Education and Research-Thiruvananthapuram, 695016 Kerala, India*
[3]*Max-Planck Institute for Chemical Physics of Solids, D-01187 Dresden, Germany*
(Received 11 October 2010; published 13 January 2011)

^{31}P nuclear and muon spin-lattice relaxation-rate measurements in $SrZnVO(PO_4)_2$, a $S = 1/2$ frustrated magnet on a square lattice, are presented. The temperature (T) dependence of the in-plane correlation length ξ is derived and it is shown that the overall behavior is analogous to the one found for nonfrustrated systems but with a reduced spin stiffness. The temperature dependence of ξ in $SrZnVO(PO_4)_2$ is compared to the one of other frustrated magnets on a square lattice with competing nearest neighbor (J_1) and next-nearest-neighbor (J_2) exchange couplings and it is shown that ξ progressively decreases as the ratio J_2/J_1 approaches the critical value leading to the suppression of long-range magnetic order. In spite of the differences in the functional form of $\xi(T)$ found in different vanadates, it is pointed out that the characteristic energy scale describing spin correlations in all those compounds appears to scale as $|2J_2 + J_1|$.

DOI: 10.1103/PhysRevB.83.014412 PACS number(s): 76.60.Es, 76.75.+i, 75.10.Jm, 75.40.Gb

I. INTRODUCTION

The study of quantum magnetism has received a renewed attention after the discovery of high-temperature superconductivity in the cuprates. In fact, these materials have made it possible to investigate at the experimental level the phase diagram of $S = 1/2$ Heisenberg antiferromagnets on a square lattice with great accuracy.[1] The behavior of the correlation length has been derived by means of neutron-scattering experiments[2] and nuclear spin-lattice relaxation-rate measurements;[3,4] the form of the dynamical susceptibility and, accordingly, the value of the scaling exponents which characterize those systems have been obtained.[5] More recently, much attention has been addressed to the investigation of frustrated square-lattice (FSL) systems where the frustration is induced by a next-nearest-neighbor (n.n.n.) exchange coupling J_2 competing with the nearest-neighbor (n.n.) one (J_1) along the side of the square.[6] Frustration is expected to further enhance quantum fluctuations and to lead to the suppression of long-range magnetic order for certain values of the ratio $r = J_2/J_1$. In particular, when both exchange couplings are antiferromagnetic for $r \simeq 0.5$, a spin-liquid ground state is expected,[7] while when J_1 is ferromagnetic (i.e., $J_1 < 0$) for $r \simeq -0.5$, a nematic order for the two-spin correlation function is envisaged.[8,9] The J_1-J_2 model on a square lattice has received renewed attention in the past two years when it was realized that the parent compounds of the recently discovered iron-based superconductors are characterized by comparable n.n. and n.n.n. hopping integrals, which may yield competing exchange couplings within the square lattice formed by iron atoms.[10] In fact, those materials would represent an extension of the J_1-J_2 model on a square lattice to itinerant electron systems. With regard to the insulating systems, a number of compounds have been recently identified to be prototypes of FSL systems and investigated through different experimental approaches.[6,11–16] Attempts have been made to theoretically understand their high field properties[11,17] and the exchange mechanisms.[18] Despite such theoretical and experimental progress, a number of key questions still have to be addressed. For example, the parts of the phase diagram where long-range order should be absent have not been studied so far; moreover it is not clear how the temperature dependence of the in-plane correlation length ξ changes with r. Unfortunately, it is not possible to address this latter aspect by means of inelastic neutron scattering experiments since only small crystals are available for the prototypes of the J_1-J_2 model on a square lattice.[6] Hence, it would be worthwhile to find other experimental techniques which could determine the effect of frustration on ξ.

Here we present an experimental study of the temperature (T) dependence of the in-plane correlation length ξ, derived by means of nuclear and muon spin-lattice relaxation rates, in $SrZnVO(PO_4)_2$ (Fig. 1), a prototype of a frustrated magnet on a square lattice with competing ferromagnetic n.n. and antiferromagnetic n.n.n. couplings. It is shown that ξ diverges exponentially on cooling with a reduced spin stiffness, possibly scaling as $|J_1 + 2J_2|$. A comparison with the results previously obtained by our group on other systems with $r < 0$ appears to qualitatively support this scaling of the spin stiffness, even if an accurate description of ξ on approaching the transition to the columnar ground state should take into account the spin anisotropy and interlayer couplings.

II. TECHNICAL ASPECTS AND EXPERIMENTAL RESULTS

The synthesis of a $SrZnVO(PO_4)_2$ polycrystalline sample was carried out by using the protocol reported in Refs. 16 and 19. Direct-current magnetization (M) measurements were performed in order to estimate the superexchange coupling constants for our sample and to check if they are consistent with the ones reported in the literature.[11,16,18] The T dependence of the static uniform spin susceptibility $\chi = M/H$,[20] with H the magnetic field intensity, was analyzed by fitting the high-T data to Curie-Weiss law and to the high-T series expansion.[21] It was found that $J_1 = -7.53 \pm 0.7$ K and $J_2 = 8.63 \pm 0.6$ K, values which are quite consistent with the ones previously reported in the literature.[11,16,18] In the

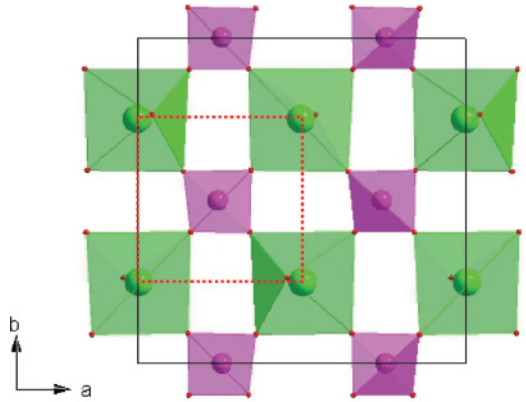

FIG. 1. (Color online) Projection of $SrZnVO(PO_4)_2$ structure along the c axis evidencing the planes containing V^{4+} ions. Vanadium ions are in green (large circles), phosphorus in purple (medium circles), and oxygen ions in red (small circles). VO_5 pyramids and $P1O_4$ tetrahedra are also visible. The red dotted square shows the $S = 1/2$ square lattice.

following, in order to better compare $SrZnVO(PO_4)_2$ to the other systems, we introduce a characteristic energy scale $J_C = \sqrt{J_1^2 + J_2^2} \simeq 11.45$ K, which provides the magnitude of the exchange couplings.

^{31}P NMR measurements were carried out by using standard radio-frequency (rf) pulse sequences. At low field, where the full spectrum could be irradiated, the NMR powder spectra were obtained from the Fourier transform of half of the echo after a $\pi/2$-τ_E-π pulse sequence. The NMR powder spectrum Fig. 2(a) was characterized by an asymmetric line shape, quite similar to the one found by Nath *et al.*[22] in the isostructural $Pb_2VO(PO_4)_2$ compound. The narrow central component is associated with P2 sites lying in between adjacent vanadium layers, while the broader component to the P1 site (Fig. 1) which lies within vanadium layers and is characterized by a larger hyperfine coupling. At high magnetic fields the line broadening prevented the irradiation of the whole line and the NMR spectrum had to be derived either by recording the intensity of the signal upon making discrete frequency steps or upon sweeping the magnetic field [Fig. 2(a)]. The T dependence of the NMR shift ΔK for the P1 site for $\mathbf{H} \parallel c$ and $\mathbf{H} \parallel ab$ was determined by recording the position of the low-frequency (high-field) and of the high-frequency (low-field) shoulders of the NMR spectrum, respectively, as a function of T. Both quantities were found to scale linearly with χ but with opposite slopes, indicating an opposite sign in the hyperfine coupling components [Fig. 2(b)].

Nuclear spin-lattice relaxation rate $1/T_1$ was derived from the recovery of the nuclear magnetization after a saturating pulse sequence. In view of the anisotropy of the hyperfine coupling tensor $1/T_1$ depends on the portion of the spectrum being irradiated. Since the low-frequency (high-field) shoulder of the ^{31}P1 spectrum was more separated from the rest of the spectra we have decided to irradiate just that part of ^{31}P NMR powder spectrum, corresponding to the crystallites with $\mathbf{H} \parallel c$. From now on we refer to T_1 only for the ^{31}P1 site and for that orientation. The corresponding recovery laws for the nuclear magnetization could be nicely fit by a single exponential. In Fig. 3 the temperature dependence of $1/T_1$ in the 1.6 K–100 K

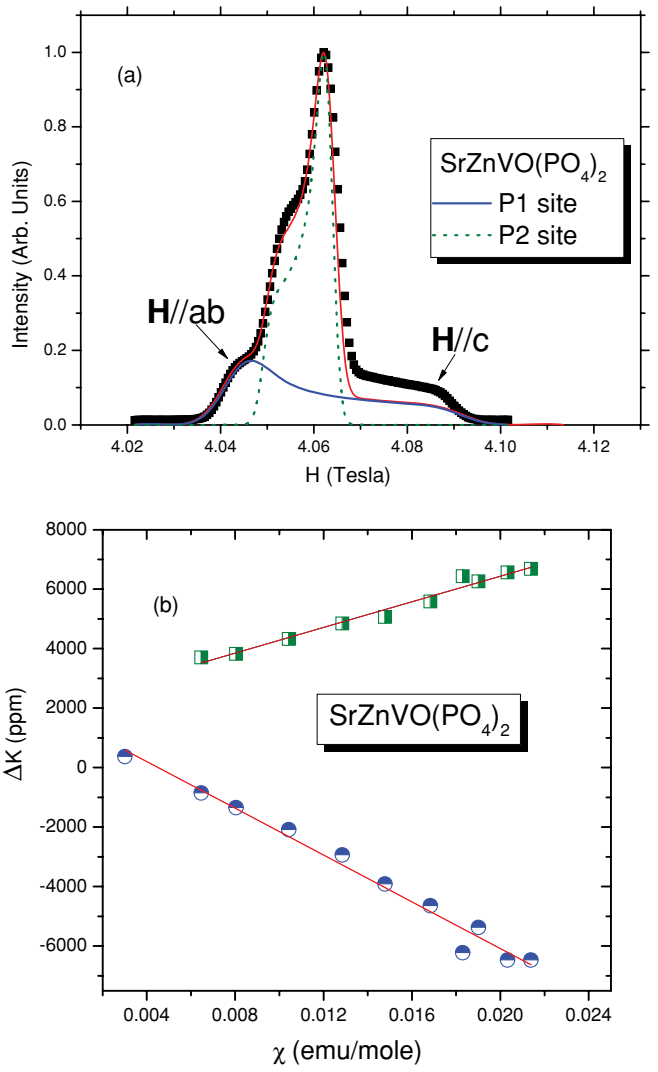

FIG. 2. (Color online) (a) Field-swept ^{31}P NMR spectrum reported for rf irradiation at $\nu = 70$ MHz. The contribution from ^{31}P1 and ^{31}P2 sites is evidenced and the parts of ^{31}P1 spectra corresponding to an orientation of the grains with $\mathbf{H} \parallel c$ or $\mathbf{H} \parallel ab$ are shown. (b) The ^{31}P NMR shift of the high (green squares) and low (blue circles) frequency shoulders of ^{31}P1 NMR spectra, corresponding to $\mathbf{H} \parallel ab$ and $\mathbf{H} \parallel c$, respectively, is reported as a function of the macroscopic spin susceptibility with the temperature as an implicit parameter.

range is shown. At high temperature $1/T_1$ is flat, then it smoothly decreases and eventually it shows a well-defined peak at $T_C = 2.65 \pm 0.02$ K, corresponding to the columnar ordering temperature. Below T_C a rapid decrease of $1/T_1$ is observed. This behavior is very similar to the one reported by Nath *et al.*[22] for $Pb_2VO(PO_4)_2$. No significant change in $1/T_1$ was noticed upon increasing the magnetic field intensity from 7 to 35 kG (Fig. 3) at high T. On the other hand, a tiny change has to be expected for $T \to T_C$ due to the variation of the transition temperature with the field.[22]

Muon spin resonance (μSR) measurements were performed at the ISIS pulsed muon source on the MuSR beam line. In zero field (ZF), for $T > T_C$, the decay of the muon asymmetry was characterized by a stretched exponential function

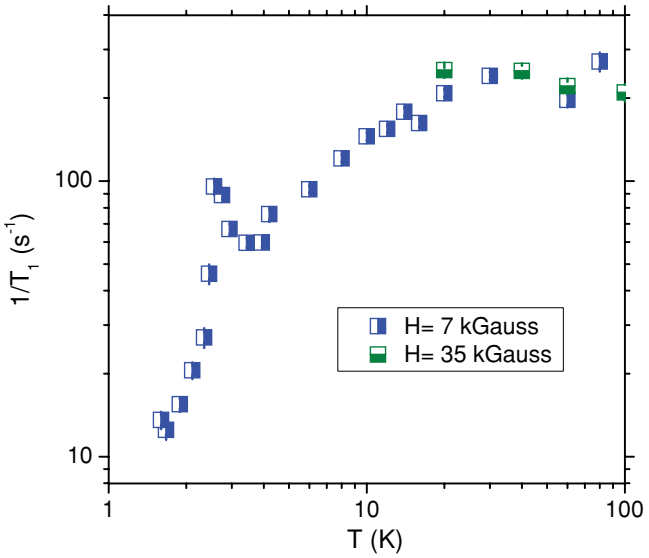

FIG. 3. (Color online) Temperature dependence of ^{31}P1 nuclear spin-lattice relaxation rate in $SrZnVO(PO_4)_2$, for $\mathbf{H} \parallel c$.

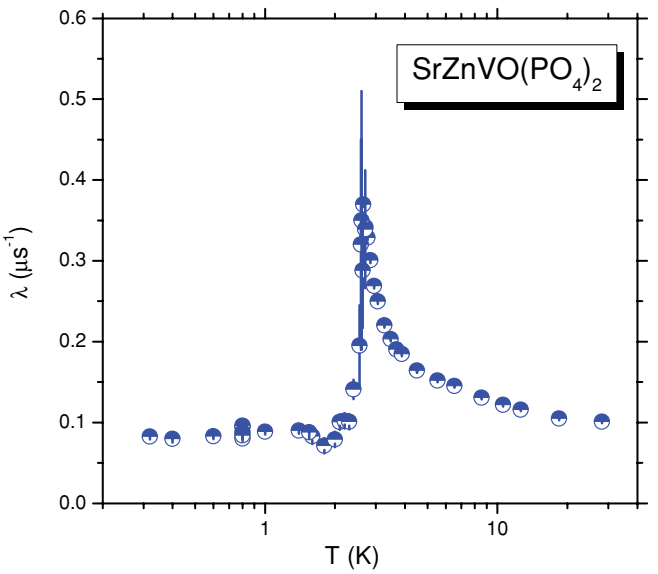

FIG. 4. (Color online) Temperature dependence of the zero-field muon relaxation rate in $SrZnVO(PO_4)_2$.

$A(t) = A(0)\exp[-(\lambda t)^{\beta}]$,[20] with β progressively decreasing from 0.7 to 0.5 upon decreasing the temperature from 30 K to T_C. The stretched exponential character of the relaxation can be associated either with a distribution of muon sites or with an anisotropic hyperfine coupling, yielding to a distribution of relaxation rates in a powder sample. Below T_C clear oscillations are observed in ZF,[20] showing that there is a spontaneous sublattice magnetization causing a nonzero magnetic field B_μ at the muon site.[23] Accordingly, the decay of the muon asymmetry followed the behavior typically found for powder samples in ZF,[24]

$$A(t) = A_1 e^{-\sigma t}\cos(\gamma_\mu B_\mu t + \phi) + A_2 e^{-\lambda t} + B, \qquad (1)$$

where γ_μ is the muon gyromagnetic ratio, σ the decay rate of the oscillating part, mostly due to a inhomogeneous distribution of the local field at the muon sites, while B is a constant background arising from the sample environment.

The temperature dependence of λ and of B_μ derived from the fit of the asymmetry with the aforementioned expressions is reported in Figs. 4 and 5, respectively.

III. DISCUSSION

First we shall consider the temperature dependence of the order parameter, as derived from ZF μSR measurements. The local field at the muon can be written

$$B_\mu = \sum_i A_i^\mu \langle \vec{S}_i \rangle = A_{\rm eff}^\mu |\langle \vec{S} \rangle|, \qquad (2)$$

where A_i^μ is the hyperfine coupling between the muon and the ith V^{4+} spin. Since the magnitudes of all V^{4+} spins $|\langle \vec{S} \rangle|$ are expected to be the same, the local field at the muon can be written in terms of an effective total hyperfine coupling $A_{\rm eff}^\mu$ times $|\langle \vec{S} \rangle|$. Hence, the T dependence of the local field at the muon gives directly the one of the sublattice magnetization. With regard to the critical behavior of the order parameter for $T \to T_c$, here we only remark that the critical exponent β can be consistent with the one expected for finite two-dimensional (2D) XY systems ($\beta = 0.235$)[25] found in other similar vanadates.[22,23,26] Nevertheless, the accuracy of the experimental points does not allow one to give a definite answer in this respect. On the other hand, the low-temperature behavior of B_μ provides information on the dispersion relation for the spin-wave excitations. The reduction of the low-temperature sublattice magnetization is consistent with a power law $|\langle \vec{S} \rangle|(T) \sim T^n$, with $n = 1.8 \pm 0.4$. Although this value would be consistent with the

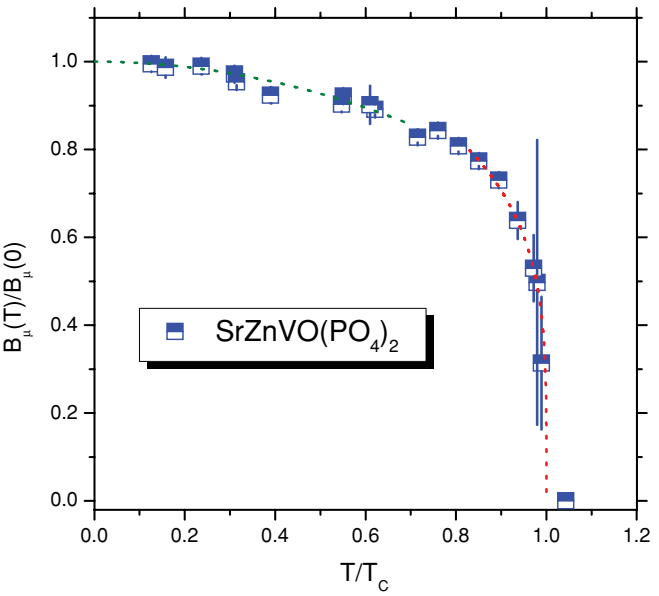

FIG. 5. (Color online) The local field at the muon, normalized to its low-temperature value $B_\mu = 186 \pm 3$ G, reported as a function of T/T_c, with $T_c = 2.65$ K. The low-temperature blue dotted line shows the behavior expected for a power-law reduction of $B_\mu(T) = B_\mu(0)(1 - aT^2)$. The high-temperature red dotted line shows the critical behavior for $T \to T_c$ for a critical exponent $\beta = 0.235$, as is expected for a 2D XY model.

dispersion relation for nearly 2D antiferromagnets,[27] it is difficult to give a precise statement in view of the experimental uncertainty. Nevertheless, as is shown at the end of this section, the T dependence of $1/T_1$ also seems to support the 2D character of the spin-wave excitations, with a quasilinear magnon dispersion.

Now we turn to the discussion of the temperature dependence of ^{31}P nuclear spin-lattice relaxation rate, which makes it possible to derive information on the low-energy dynamics and on the spin correlations. In the case of a magnetic relaxation process driven by electron spin fluctuations, $1/T_1$ can be written[28]

$$\frac{1}{T_1} = \frac{\gamma^2}{2N} \sum_{\alpha,\mathbf{q}} [|A_{\mathbf{q}}|^2 S_{\alpha,\alpha}(\mathbf{q},\omega_L)]_{\perp}, \tag{3}$$

where γ is the nuclear gyromagnetic ratio, $|A_{\mathbf{q}}|^2$ the form factor describing the hyperfine coupling with spin excitations at wave vector $\mathbf{q}$ and $S_{\alpha,\alpha}(\mathbf{q},\omega_L)$ ($\alpha = x,y,z$) the component of the dynamical structure factor at the Larmor frequency ω_L. The $\perp$ subscript indicates that one should consider the components of the fluctuating hyperfine field perpendicular to the quantization axis, given by the direction of the static external field. By using scaling arguments, it is possible to write the dynamical structure factor in terms of the in-plane correlation length ξ (in lattice units hereafter) and establish a one-to-one relationship between $1/T_1$ and ξ. This procedure has proven to be very useful to study the temperature dependence of the correlation length in the cuprates, which are prototypes of 2D $S = 1/2$ Heisenberg antiferromagnets on a square lattice,[4] and to determine experimentally the value of the dynamical scaling exponent $z = 1$. Given the similarity between the cuprates and the vanadates under investigation, we use the same approach here to derive ξ from ^{31}P $1/T_1$, assuming $z = 1$. Although deviations from $z = 1$ would affect the estimate of the absolute value of ξ, the basic functional form $\xi(T)$ would be only slightly affected. Accordingly, one can write[4]

$$\frac{1}{T_1} \simeq \gamma^2 \frac{S(S+1)}{3} \xi^{z+2} \frac{\beta(\xi)^2 \sqrt{2\pi}}{\omega_E} \frac{1}{4\pi^2} \times \int_{BZ} d\vec{q} \frac{|A_{\vec{q}}|^2}{1 + \xi^2(\vec{q} - \vec{Q}_C)^2}, \tag{4}$$

where $\beta = (4\pi^2/\xi^2)/[\int d\vec{q}/(1+q^2\xi^2)]$ is a normalization factor which makes it possible to preserve the spin sum rule[4] and $\vec{Q}_C$ is the columnar critical wave vector. $\omega_E = (J_C k_B/\hbar)\sqrt{2nS(S+1)/3}$ is the Heisenberg exchange frequency,[28] with $n = 4$ the number of n.n. and of n.n.n..

In order to establish a one-to-one relationship between $1/T_1$ and ξ, from the preceding equation one has first to derive the hyperfine coupling tensor components and the form factor for the ^{31}P1 site. The components of the hyperfine tensor can be derived from the plot of the shift ΔK for the magnetic field along the α direction vs the molar macroscopic susceptibility χ [Fig. 2(b)], which is assumed to be isotropic. Then one can write

$$\Delta K_\alpha = \frac{A_{\alpha\alpha}\chi}{g\mu_B N_A}, \tag{5}$$

with μ_B the Bohr magneton and N_A the Avogadro's number.

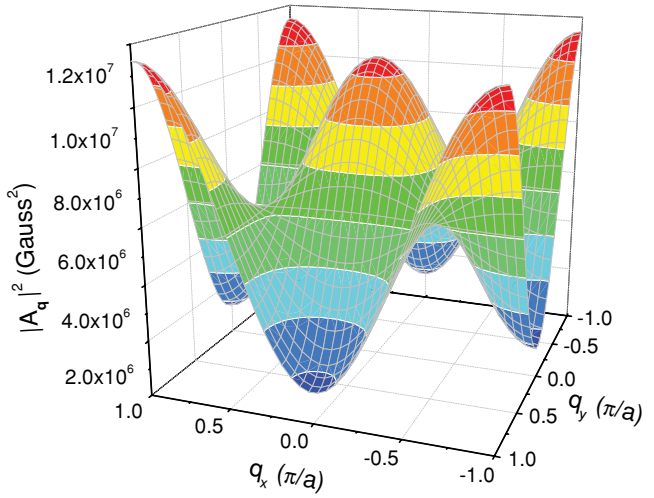

FIG. 6. (Color online) The form factors for the ^{31}P1 site reported as a function of the in-plane components (q_x and q_y) of the wave vector of the spin excitations for $SrZnVO(PO_4)_2$.

For $SrZnVO(PO_4)_2$ one finds $A_{cc} = -4300 \pm 190$ G and $A_{aa} \simeq A_{bb} = 2360 \pm 200$ G. In fact, since the measurements on powders did not allow one to discern between ΔK_a and ΔK_b we have assumed $A_{aa} \simeq A_{bb}$. In $Pb_2VO(PO_4)_2$, on the other hand, a small difference between those two components is observed.[22] The total hyperfine tensor is the sum of a transferred term A^t and of a dipolar term A^d. The latter one can be calculated on the basis of lattice sums, while the former one is assumed to be the sum of four equal terms arising from the hyperfine coupling between ^{31}P1 nuclei and the four n.n. V^{4+} spins. Hence, the contribution to the transferred hyperfine term is simply given by $A^t = (A - A^d)/4$. Now that both the transferred and the dipolar coupling between ^{31}P1 nucleus and each V^{4+} spin are known, it is possible to derive the hyperfine form factor. The form factor of $SrZnVO(PO_4)_2$ is reported in Fig. 6. It is noticed that, owing to the symmetry position of P1 site, the form factor shows a nonvanishing minimum at $\vec{Q}_C = (\pm\pi,0)$ and $(0,\pm\pi)$. This explains why $1/T_1$ progressively decreases as the system gets more correlated upon decreasing temperature (Fig. 3) and why only when the correlation length is sufficiently large does $1/T_1$ increase again. In fact, from Eq. (4) it is possible to derive numerically the behavior of $1/T_1$ vs ξ (Fig. 7) and one finds a minimum for $\xi \simeq 5$ lattice steps. Accordingly, from the experimental data reported in Fig. 3 it is now possible to derive quantitatively the temperature dependence of ξ in $SrZnVO(PO_4)_2$.

In order to derive the temperature dependence of ξ from $\lambda(T)$ one has first to subtract the T-independent dipolar contribution from the raw data in Fig. 4 and then proceed in the same way as was done for $1/T_1$. However, here the form factor cannot be determined since the muon site and hyperfine couplings are unknown. It is noticed that, at variance with P1 site, the muon should not be in a position symmetrical with respect to the neighboring V^{4+} ions, since λ continues to diverge upon cooling. Thus, if no filtering effect due to the form factor is present, one can safely write $\lambda \sim \xi$, for $\xi \gg 1$.[4] Namely, the temperature dependence of λ directly gives the one of ξ although, unlike ^{31}P $1/T_1$, λ does not make it possible to estimate quantitatively ξ. Nevertheless, by matching the $\xi(T)$

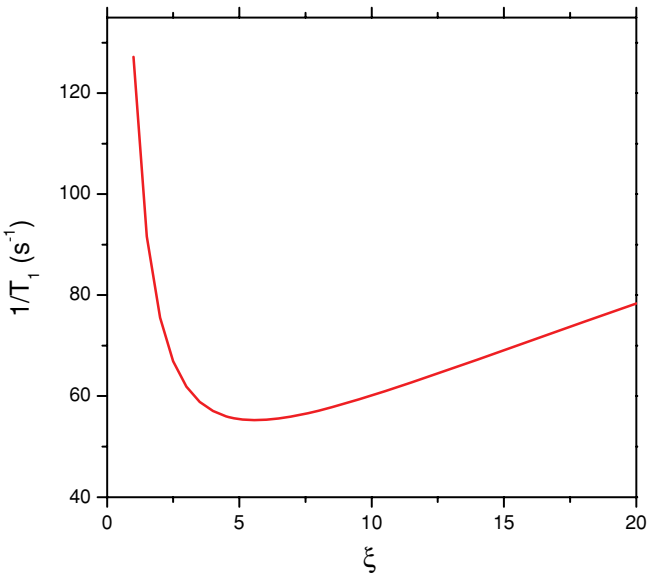

FIG. 7. (Color online) ^{31}P1 nuclear spin-lattice relaxation rate in $SrZnVO(PO_4)_2$ reported as a function of the in-plane correlation length (in lattice units) according to Eq. (4) in the text.

derived from $\lambda(T)$ with the one quantitatively derived from $1/T_1$ over the same T range, it is possible to use also $\lambda(T)$ data to estimate quantitatively $\xi(T)$.

In Fig. 8 we report the temperature dependence of ξ derived by means of ^{31}P1 $1/T_1$ and the one obtained by means of $\lambda(T)$ in a temperature range where ξ is sufficiently large so that either Eq. (4) applies or $\lambda \sim \xi$. One notices an overall good agreement in the behavior of $\xi(T)$ derived through both methods; moreover, it is noticed that ξ diverges exponentially on decreasing temperature. For a nonfrustrated $S = 1/2$ Heisenberg antiferromagnet on a square lattice one

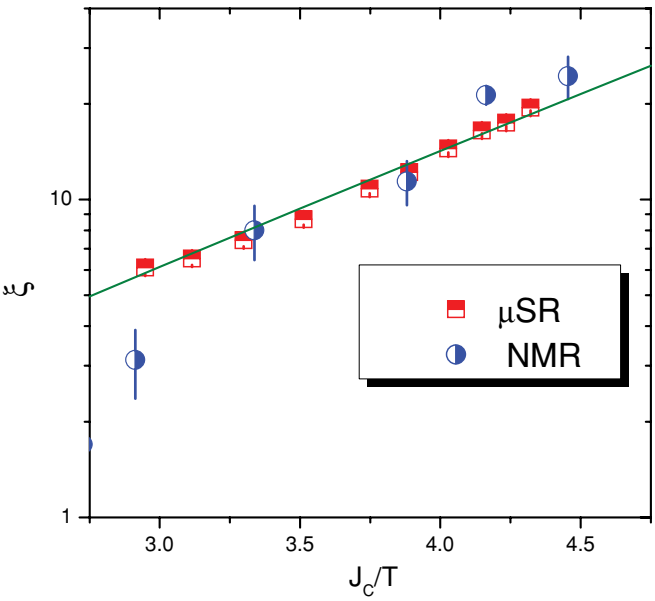

FIG. 8. (Color online) The temperature dependence of the in-plane correlation length (in lattice units) derived from λ and $1/T_1$ data reported as a function of J_C/T. The solid line shows the behavior expected for a spin stiffness $\rho_s = 0.79 \pm 0.05 \times 1.15 J_C/2\pi$.

would expect that $\xi(T) \simeq \exp(2\pi\rho_s/T)/(T + 4\pi\rho_s)$,[29] with ρ_s the spin stiffness, which for nonfrustrated systems turns out to be $\rho_s \simeq 1.15 J_C/2\pi$. Here we find that the behavior of $\xi(T)$ is the same but with a reduced effective spin stiffness constant. In fact, the data in Fig. 8 can be nicely fit with $\rho_s = 0.79 \pm 0.05 \times 1.15 J_C/2\pi = 1.66 \pm 0.1$ K.

Recently, Härtel *et al.*[30] have calculated the temperature dependence of $\xi(T)$ for $J_2 \leqslant 0.44|J_1|$ (i.e., $r \geqslant -0.44$), namely, for the part of the phase diagram adjacent to the one experimentally investigated here and in Ref. 23. They found that $\xi(T)$ diverges exponentially with decreasing temperature with an effective spin stiffness $\rho_s \simeq -(J_1 + 2J_2)/8$, which vanishes on approaching $r \simeq -0.5$, namely, the region with no long-range magnetic order.[30] $SrZnVO(PO_4)_2$, however, is characterized by $r \simeq -1.15$ and it is not clear if the previous expression for the spin stiffness can still be used. Nevertheless, if one considers that also for the compounds with $r \leqslant -0.5$ an analogous expression $\rho_s \simeq +(J_1 + 2J_2)/8$ could hold, one would derive for $SrZnVO(PO_4)_2$ an effective spin stiffness $\rho_s = 1.23 \pm 0.16$ K, a value which is close to the one experimentally determined here (Fig. 8). Accordingly, in the absence of a theoretical calculation, one would be tempted to argue that on both sides of the critical point around $r \simeq -0.5$ the correlation length diverges exponentially on cooling with an effective spin stiffness $\rho_s \simeq |(J_1 + 2J_2)/8|$, progressively vanishing as $r \to 0.5$.

Now, it is rather interesting to compare the behavior of ξ in $SrZnVO(PO_4)_2$ with the one in $BaCdVO(PO_4)_2$ ($r \simeq -0.9$[15]) and in $Pb_2VO(PO_4)_2$ ($r \simeq -1.8$[31]), derived from the temperature dependence of $\lambda(T)$.[23] Since in the latter two compounds it was not possible to determine the absolute value of ξ, we assumed that $\lambda \sim \xi$ and rescaled the values of λ

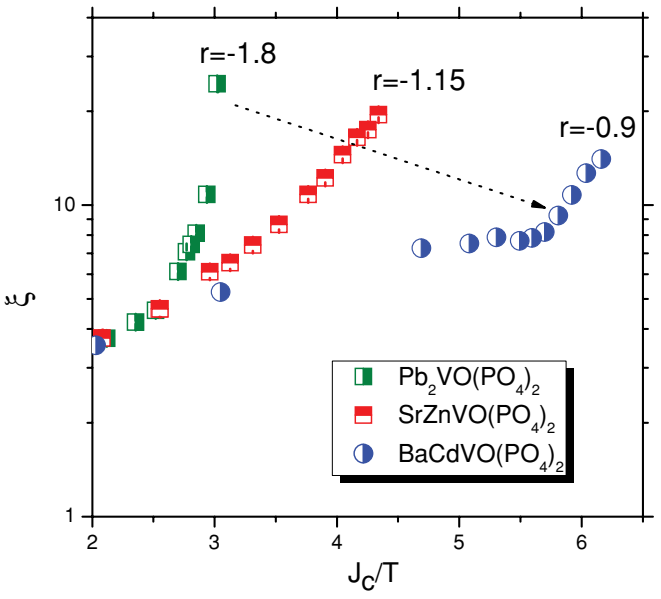

FIG. 9. (Color online) The temperature dependence in-plane correlation length derived from λ reported vs J_C/T compared to the one derived for $SrZnVO(PO_4)_2$ ($J_C = 11.45$ K), $BaCdVO(PO_4)_2$ ($J_C = 4.8$ K)[15], and $Pb_2VO(PO_4)_2$ ($J_C = 10.7$ K).[31] The dotted arrow points out that upon decreasing $|J_2/J_1|$ the correlation length increases less rapidly on cooling.

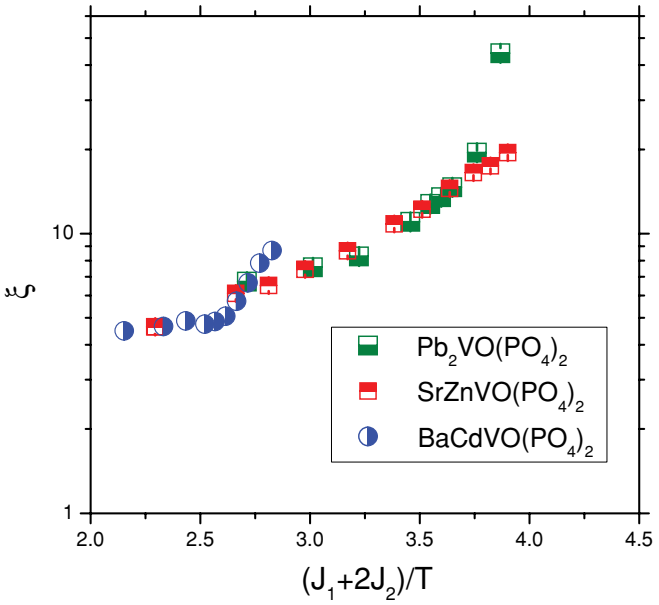

FIG. 10. (Color online) The in-plane correlation length derived from $\lambda(T)$ reported as a function of $(J_1 + 2J_2)/T$ for $SrZnVO(PO_4)_2$ [$(J_1 + 2J_2) = 9.73$ K], $BaCdVO(PO_4)_2$ [$(J_1 + 2J_2) = 2.8$ K)],[15,32] and $Pb_2VO(PO_4)_2$ [$(J_1 + 2J_2) = 13.7$ K].[31]

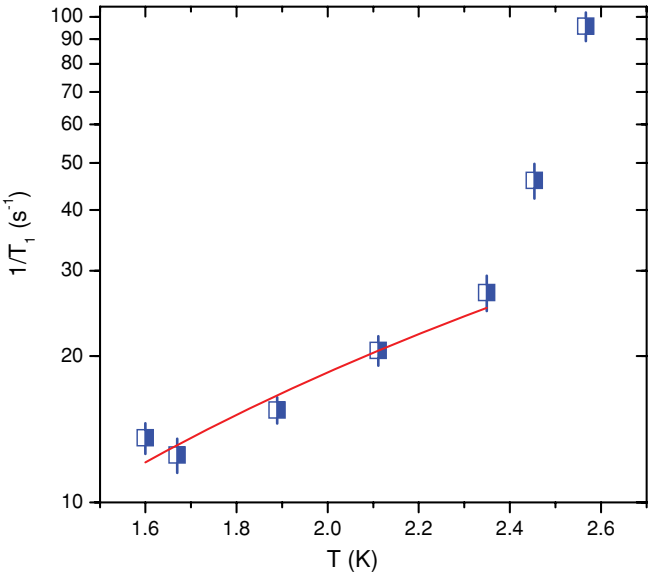

FIG. 11. (Color online) The temperature dependence of ^{31}P1 $1/T_1$ in $SrZnVO(PO_4)_2$ in the columnar ground state is reported. The solid line shows the best fit according to a power-law behavior $1/T_1 \sim T^b$ with $b = 1.9 \pm 0.3$.

so that for $T \simeq J_C/2$, when $\xi \to 1$, ξ is the same in all compounds. The corresponding data are reported in Fig. 9. One notices that indeed ξ decreases as $r \to -0.5$; however, it is also noticed that while for $SrZnVO(PO_4)_2$ the correlation length diverges exponentially over a wide T range, this is not the case for the other two systems. In fact, it has been pointed out that the behavior of $Pb_2VO(PO_4)_2$ is more characteristic of a 2D XY system,[23] while in $BaCdVO(PO_4)_2$ possible nematic correlations appear, leading to a logarithmic increase of ξ on cooling.[23] Moreover, deviations associated with the critical behavior are observed on approaching T_C. Hence, it appears that although in general the system becomes less correlated as $r \to -0.5$ the correct analytical form of the correlation function is not simply exponential and that details taking into account the presence of a possible XY character or of nematic correlations should be considered. Nevertheless, it is interesting to observe that in spite of the functional form, the characteristic energy scale describing the growth of the in-plane correlation length appears to scale as $J_1 + 2J_2$ far from T_C. In fact, if one now plots the ξ data when $\xi \gg 1$ for the different compounds as a function of $(J_1 + 2J_2)/T$, one observes a reasonable overlap between the data of the different compounds until when the XY character or the interlayer coupling do not give rise to a critical enhancement of the correlations on approaching T_C (see Fig. 10). It is noticed that also in this plot the magnitude of ξ in $Pb_2VO(PO_4)_2$ and $BaCdVO(PO_4)_2$ has been rescaled in order to match the one quantitatively derived for $SrZnVO(PO_4)_2$. Hence, a definite answer on the validity of the scaling would require an independent quantitative estimate of ξ also for those two compounds.

Finally, we discuss the behavior of the spin-lattice relaxation rate in the magnetically ordered columnar phase. Below T_C one observes a marked decrease of $1/T_1$ which in the low-temperature limit should be ascribed to the vanishing of the two-magnon Raman relaxation processes.[33] If the gap in the magnon dispersion curve is negligible, one would expect a power-law behavior of $1/T_1$ with a power-law exponent depending on the magnetic lattice dimensionality and on the analytical form of the magnon dispersion curve.[33] In case of a linear dispersion curve, neglecting the presence of a gap in the spin-wave dispersion, for a quasi-2D system one would expect $1/T_1 \sim T^2$. Here we find that $1/T_1 \sim T^b$ with $b = 1.9 \pm 0.3$ (see Fig. 11), in reasonable agreement with the theoretical expectations and with the behavior of the sublattice magnetization derived from μ^+SR measurements.

IV. CONCLUSIONS

In conclusion, we have determined quantitatively the temperature dependence of the in-plane correlation length ξ in $SrZnVO(PO_4)_2$, a frustrated $S = 1/2$ magnet on a square lattice with $r \simeq -1.15$, by means of nuclear and muon spin-lattice relaxation-rate measurements. It has been shown that ξ diverges exponentially on cooling with a reduced spin stiffness, which appears to roughly scale as $|J_1 + 2J_2|$. A comparison with the results previously obtained by our group on other systems with $r < 0$ appears to support this scaling of the spin stiffness even if an accurate description of ξ on approaching the transition to the columnar ground state should take into account the spin anisotropy and interlayer couplings.

ACKNOWLEDGMENTS

The technical assistance by Sean Giblin during the measurements at ISIS is gratefully acknowledged. The research activity in Pavia was supported by Fondazione Cariplo (Grant No. 2008-2229) research funds.

[1]E. Dagotto, Rev. Mod. Phys. **66**, 763 (1994); D. C. Johnston, in *Handbook of Magnetic Materials*, edited by K. H. J. Buschow (Elsevier Science, New York, 1997), Vol. 10.

[2]B. Keimer, N. Belk, R. J. Birgeneau, A. Cassanho, C. Y. Chen, M. Greven, M. A. Kastner, A. Aharony, Y. Endoh, R. W. Erwin, and G. Shirane, Phys. Rev. B **46**, 14034 (1992).

[3]T. Imai, C. P. Slichter, K. Yoshimura, and K. Kosuge, Phys. Rev. Lett. **70**, 1002 (1993).

[4]P. Carretta, A. Rigamonti, and R. Sala, Phys. Rev. B **55**, 3734 (1997); P. Carretta, T. Ciabattoni, A. Cuccoli, E. Mognaschi, A. Rigamonti, V. Tognetti, and P. Verrucchi, Phys. Rev. Lett. **84**, 366 (2000).

[5]M. Greven, R. J. Birgeneau, Y. Endoh, M. A. Kastner, B. Keimer, M. Matsuda, G. Shirane, and T. R. Thurston, Phys. Rev. Lett. **72**, 1096 (1994).

[6]P. Carretta, N. Papinutto, R. Melzi, P. Millet, S. Gouthier, P. Mendels, and P. Wzietek, J. Phys. Condens. Matter **16**, S849 (2004); A. Bombardi, J. Rodriguez-Carvajal, S. Di Matteo, F. de Bergevin, L. Paolasini, P. Carretta, P. Millet, and R. Caciuffo, Phys. Rev. Lett. **93**, 027202 (2004).

[7]P. Chandra, P. Coleman, and A. I. Larkin, Phys. Rev. Lett. **64**, 88 (1990); C. Weber, L. Capriotti, G. Misguich, F. Becca, M. Elhajal, and F. Mila, *ibid.* **91**, 177202 (2003).

[8]N. Shannon, T. Momoi, and P. Sindzingre, Phys. Rev. Lett. **96**, 027213 (2006).

[9]N. Shannon, B. Schmidt, K. Penc, and P. Thalmeier, Eur. Phys. J. B **38**, 599 (2004).

[10]H. Lee, Y.-Z. Zhang, H. O. Jeschke, and R. Valentí, Phys. Rev. B **81**, 220506 (2010); B. Schmidt, M. Siahatgar, and P. Thalmeier, *ibid.* **81**, 165101 (2010); Q. Si and E. Abrahams, Phys. Rev. Lett. **101**, 076401 (2008).

[11]A. A. Tsirlin, B. Schmidt, Y. Skourski, R. Nath, C. Geibel, and H. Rosner, Phys. Rev. B **80**, 132407 (2009).

[12]A. A. Tsirlin, R. Nath, A. M. Abakumov, R. V. Shpanchenko, C. Geibel, and H. Rosner, Phys. Rev. B **81**, 174424 (2010).

[13]A. A. Tsirlin, A. A. Belik, R. V. Shpanchenko, E. V. Antipov, E. Takayama-Muromachi, and Helge Rosner, Phys. Rev. B **77**, 092402 (2008).

[14]M. Skoulatos, J. P. Goff, C. Geibel, E. E. Kaul, R. Nath, N. Shannon, B. Schmidt, A. P. Murani, P. P. Deen, M. Enderle, and A. R. Wildes, Europhys. Lett. **88**, 57005 (2009).

[15]R. Nath, A. A. Tsirlin, H. Rosner, and C. Geibel, Phys. Rev. B **78**, 064422 (2008).

[16]E. E. Kaul, Ph.D. thesis, Technical University Dresden, 2005; electronic version available at [http://hsss.slub-dresden.de/documents/1131439690937-4924/1131439690937-4924.pdf].

[17]P. Thalmeier, M. E. Zhitomirsky, B. Schmidt, and N. Shannon, Phys. Rev. B **77**, 104441 (2008); B. Schmidt, P. Thalmeier, and N. Shannon, *ibid.* **76**, 125113 (2007).

[18]A. A. Tsirlin and H. Rosner, Phys. Rev. B **79**, 214417 (2009).

[19]S. Meyer, B. Mertens, and H. Muller-Buschbaum, Z. Naturforsch. B: Chem. Sci. **52**, 985 (1997).

[20]See supplemental material at [http://link.aps.org/supplemental/10.1103/PhysRevB.83.014412] for the temperature dependence of the susceptibility and for the decay of the muon asymmetry above and below T_C.

[21]H. Rosner, R. R. P. Singh, W. H. Zheng, J. Oitmaa, and W. E. Pickett, Phys. Rev. B **67**, 014416 (2003).

[22]R. Nath, Y. Furukawa, F. Borsa, E. E. Kaul, M. Baenitz, and C. Geibel, and D. C. Johnston, Phys. Rev. B **80**, 214430 (2009).

[23]P. Carretta, M. Filibian, R. Nath, C. Geibel, and P. J. C. King, Phys. Rev. B **79**, 224432 (2009).

[24]S. J. Blundell, Contemp. Phys. **40**, 175 (1999); P. Dalmas de Réotier, and A. Yaouanc, J. Phys. Condens. Matter **9**, 9113 (1997).

[25]S. T. Bramwell and P. C. W. Holdsworth, Phys. Rev. B **49**, 8811 (1994); J. Phys. Condens. Matter **5**, L53 (1993).

[26]P. Carretta, R. Melzi, N. Papinutto, and P. Millet, Phys. Rev. Lett. **88**, 047601 (2002).

[27]C. Bucci, P. Carretta, R. De Renzi, G. Guidi, S. G. Jang, E. Rastelli, A. Tassi, and M. Varotto, Phys. Rev. B **48**, 16769 (1993).

[28]T. Moriya, Prog. Theor. Phys. **16**, 23 (1956).

[29]S. Chakravarty, B. I. Halperin, and D. R. Nelson, Phys. Rev. B **39**, 2344 (1989).

[30]M. Härtel, J. Richter, D. Ihle, and S.-L. Drechsler, Phys. Rev. B **81**, 174421 (2010).

[31]E. E. Kaul, H. Rosner, N. Shannon, R. V. Shpanchenko, and C. Geibel, J. Magn. Magn. Mater. **272-276**, 922 (2004).

[32]Susceptibility and magnetization vs field measurements in our $BaCdVO(PO_4)_2$ sample confirmed, within the error bars, the values reported in Ref. 15.

[33]D. Beeman and P. Pincus, Phys. Rev. **166**, 359 (1968).